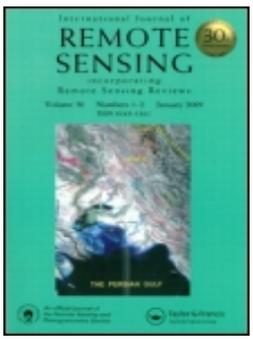

International Journal of Remote Sensing

ISSN: 0143-1161 (Print) 1366-5901 (Online) Journal homepage: http://www.tandfonline.com/loi/tres20

Intercalibration of DMSP-OLS night-time light data by the invariant region method

Jiansheng Wu , Shengbin He , Jian Peng , Weifeng Li & Xiaohong Zhong

To cite this article: Jiansheng Wu , Shengbin He , Jian Peng , Weifeng Li & Xiaohong Zhong (2013) Intercalibration of DMSP-OLS night-time light data by the invariant region method, International Journal of Remote Sensing, 34:20, 7356-7368, DOI: 10.1080/01431161.2013.820365

To link to this article: http://dx.doi.org/10.1080/01431161.2013.820365

International Journal of Remote Sensing, 2013
Vol. 34, No. 20, 7356–7368, http://dx.doi.org/10.1080/01431161.2013.820365

Taylor & Francis
Taylor & Francis Group

Intercalibration of DMSP-OLS night-time light data by the invariant region method

Jiansheng Wu[a,b], Shengbin He[a]*, Jian Peng[b], Weifeng Li[c], and Xiaohong Zhong[a]

[a]*School of Urban Planning and Design, Peking University, Shenzhen 518055, China;* [b]*College of Urban and Environmental Sciences, Peking University, Beijing 100871, China;* [c]*Department of Urban Planning and Design, The University of Hong Kong, Hong Kong, China*

(*Received 11 October 2012; accepted 11 June 2013*)

DMSP-OLS (Defense Meteorological Satellite Program Operational Linescan System) night-time light data can accurately reflect the scope and intensity of human activities. However, the raw data cannot be used directly for temporal analyses due to the lack of inflight calibration. There are three problems that should be addressed in intercalibration. First, because of differences between sensors, the data are not identical even when obtained in the same year. Second, different acquisition times may lead to random or systematic fluctuations in the data obtained by satellites in different orbits. Third, a pixel saturation phenomenon also exists in the urban centres of the image. Therefore, an invariant region method was used in this article, and the relative radiometric calibration and saturation correction achieved the desired results. In the meantime, intercalibration models for each satellite year of DMSP-OLS night-time light data were produced. Finally, intercalibration accuracy was evaluated, and the intercalibration results were tested with the corresponding gross domestic product (GDP) data.

1. Introduction

DMSP (Defense Meteorological Satellite Program) flies in a sun-synchronous orbit, and OLS (Operational Linescan System) is one of the main sensors on the DMSP satellite platform. At night, the OLS sensor can detect the lowest levels of radiation, which can be four orders of magnitude lower than that detectable by other sensors (Elvidge et al., "Mapping City Lights," 1997). Because of OLS's unique night photoelectric zooming capacity, its night-time light data are often used in studying human activities. Currently, a wide range of applications of DMSP-OLS night-time light data can be found in civilian remote sensing, including the following areas: urban expansion (Lo 2002; Elvidge et al. 2007; McDonald, Kareiva, and Formana 2008), economic evaluation (Doll, Muller, and Morley 2006; Sutton, Elvidge, and Ghosh 2007; Elvidge, Sutton, et al. 2009; Ghosh et al. 2010; Raupach, Rayner, and Paget 2010; Chaturvedi, Ghosh, and Bhandari 2011), energy consumption (Chand et al. 2009; Elvidge et al. 2011), population density (Lo 2001; Amaral et al. 2006), the heat island effect (Gallo et al. 1995), and disaster assessment (Elvidge, Hobson, et al. 2001).

The data of surface regions obtained by satellite sensors are affected by many factors, such as atmospheric absorption and scattering, solar altitude angle, terrain illumination,

*Corresponding author. Email: hsb@pku.edu.cn

and sensor calibration. These factors may cause marked differences between data from the same year obtained by different satellites, as well as random fluctuations in data for consecutive years obtained by the same satellite (Zhang et al. 2006). Since DMSP-OLS night-time light data are collected by different satellites in different years, to eliminate the differences caused by these factors, relative radiometric calibration is necessary when we conduct comparative time series analysis. Moreover, major pixel saturation exists in DMSP-OLS night-time light data, which manifests as contiguous saturated pixels in urban centres (Elvidge, Ziskin, et al. 2009). This pixel saturation has the potential to distort reality, so that analysis and comparison of light data from different regions are difficult to perform. Therefore, saturation correction is also badly needed when we carry out relative radiometric calibration.

The spectral resolution of DMSP-OLS night-time light data is low, with only one band containing grey-level information. Compared with other remote-sensing data, DMSP-OLS satellite data lack the necessary information on structure, texture, and spectral characteristics, thus increasing the difficulty and error of data calibration. To date, studies on radiometric and saturation correction of DMSP-OLS night-time light data are few and far between. Elvidge, Ziskin, et al. (2009) proposed the invariant region method and selected Sicily as the mask to extract digital number (DN) values from all images and used F121999 as the reference image; then, the night-time light product known as avg_lights_x_pct from all other satellite years were adjusted to match the F121999 data range using a quadratic equation model. Naturally, they focused only on relative radiometric calibration rather than saturation correction. Liu, He, and Yang (2011) used a similar approach to correct data within China from 1992 to 2008, then extracted the urban areas and achieved satisfactory results. Zhao, Ghosh, and Samson (2012) also used a quadratic equation model, which was developed by Elvidge, Ziskin, et al. (2009), to correct DMSP-OLS data for research on Chinese electric power consumption. Raupach, Rayner, and Paget (2010) conducted saturation correction on 2003 global night-time light data and performed the linear regression analysis with GDP, energy consumption, and CO_2 emissions. Better results were achieved when compared with those before rectification. However, they only conducted analysis of regional cross-sectional data without considering time series analysis.

In regard to the intercalibration method, research questions remain regarding how to select the invariant regions and how to reduce the impacts resulting from pixel saturation. Which type of intercalibration model is the most appropriate? How should we comprehensively evaluate the accuracy of intercalibration results? Following the invariant region method proposed by Elvidge, Ziskin, et al. (2009), we planned to explore an alternative strategy and test an invariant region method to conduct relative radiometric calibration and saturation correction simultaneously on global DMSP-OLS night-time light data from 1992 to 2010 and to analyse both in cross-sectional data and the time series.

2. Data

2.1. DMSP-OLS night-time light data

Data were derived from National Oceanic and Atmospheric Administration's (NOAA's) National Geographic Data Center (NGDC). Currently, the products of 31 satellite years (Version 4) derived from six satellites (F10, F12, F14, F15, F16, and F18) from 1992 to 2010 (see Table 1) are available for downloading from NGDC (http://www.ngdc.noaa.gov/dmsp/download.html), including three kinds of annual average data: cloud-free coverage,

Table 1. Set of annual composites from several satellites for the years 1992–2010.

Year\Satellite	F10	F12	F14	F15	F16	F18
1992	F101992	–	–	–	–	–
1993	F101993	–	–	–	–	–
1994	F101994	F121994	–	–	–	–
1995	–	F121995	–	–	–	–
1996	–	F121996	–	–	–	–
1997	–	F121997	F141997	–	–	–
1998	–	F121998	F141998	–	–	–
1999	–	F121999	F141999	–	–	–
2000	–	–	F142000	F152000	–	–
2001	–	–	F142001	F152001	–	–
2002	–	–	F142002	F152002	–	–
2003	–	–	F142003	F152003	–	–
2004	–	–	–	F152004	F162004	–
2005	–	–	–	F152005	F162005	–
2006	–	–	–	F152006	F162006	–
2007	–	–	–	F152007	F162007	–
2008	–	–	–	–	F162008	–
2009	–	–	–	–	F162009	–
2010	–	–	–	–	–	F182010

average visible, and stable light. Stable light data cover cities, townships, and other lasting light emissions, and background noise has been removed. Therefore, we chose these stable light data in this study. The spatial resolution of the data is 30 arc-seconds, about one kilometre from the equator, covering the range from –180° to 180° longitude and –65° to 75° latitude, which represents the basic global coverage of human activity areas. The grey value of data ranges from 0 to 63. This means that value 0 represents the unlit area and the greater the grey value, the higher the light level of the region will be.

Additionally, the NGDC website has produced a global night-time light product for 2006 with no sensor saturation, which can be selected as the ideal reference image data (http://www.ngdc.noaa.gov/dmsp/download_radcal.html). Compared with stable light images, the radiance-calibrated image of 2006 does not include saturated pixels and has a greater range of digital number values. Bright cores of urban centres cannot be distinguished in stable light images, which always show a saturated DN value of 63. However, in the radiance-calibrated image of 2006, the urban centres will be differently expressed in digital number values.

2.2. Ancillary data

Ancillary data include data files of the 2011 world administrative divisions in shape format, which are derived from the website of Blue Marble Geographics (http://www.bluemarblegeo.com/) and global GDP statistics from 1992 to 2010 with the current (May 2012) US dollar price as the benchmark, which are derived from the World Bank (http://www.worldbank.org/).

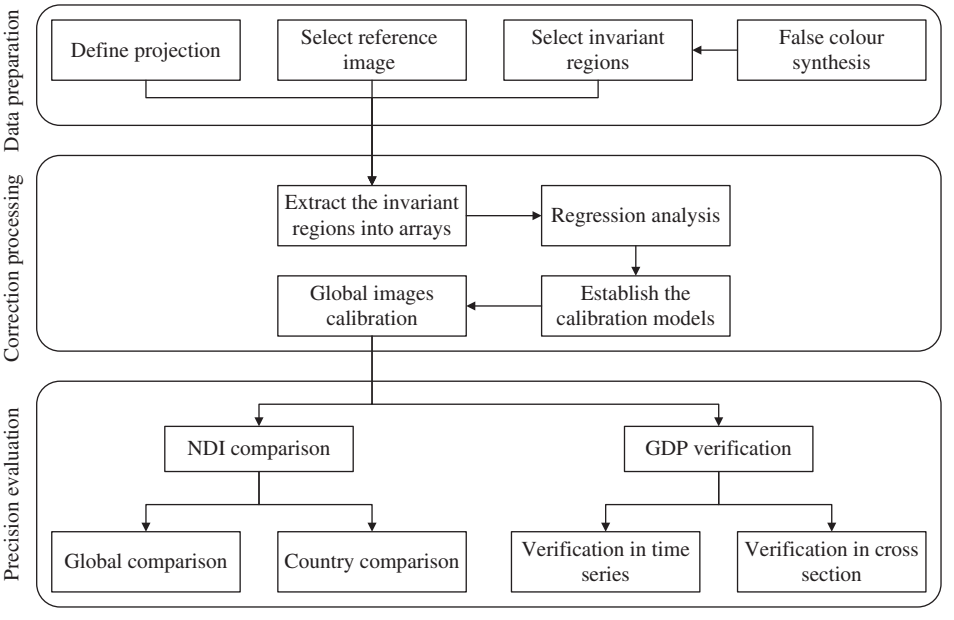

Figure 1. Flow chart of the invariant region method.

3. Methodology

Without using a large amount of satellite synchronous observation data, we can calibrate images so that the data series are comparable. We first need to define a reference image, and then gradually normalize the grey value of the multi-temporal images to the reference image (relative radiometric calibration). The invariant region method (Hall et al. 1991; Coppin and Bauer 1994; Lenney et al. 1996) first assumes that stable pixels exist in the series of images, and we can then derive their geographical sense. The invariant regions in different phases of remote-sensing images present a type of transformation relationship. After identifying the invariant regions and their transformation relation, we can carry out the relative radiometric calibration to those pending images. Since the selected reference image has been processed with radiometric calibration and there is no saturation phenomenon, the relative radiometric calibration and saturation correction of the pending image can be done simultaneously.

The flow chart of this method is shown in Figure 1.

3.1. Data preparation

The original data are in the WGS84 (World Geodetic System 1984) coordinate system and in a global latitude–longitude grid. Because the footprint of 30 arc-second grids decreases as latitude increases (Elvidge, Ziskin, et al. 2009), in order to avoid the impact of area distortion, we resampled the 30 arc-second raster image to one square kilometre grids in the Mollweide equal area projection. The reference image was a global night-time light product produced by NGDC with no sensor saturation for the year 2006, which was obtainable from the NGDC website. We derived a false colour composite using three years of images that had a greater time interval between them. The white area shown in the image is the area that remained nearly unchanged in the three phases, which is the invariant region

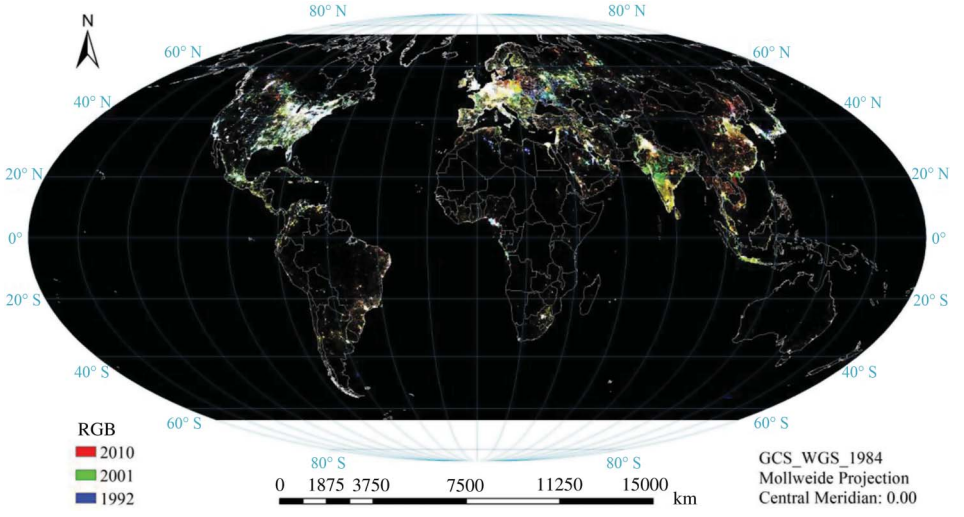

Figure 2. Colour composite image of 1992, 2001, and 2010.

we were looking for. Based on the false colour composite image (Figure 2), we selected Mauritius, Puerto Rico, and Okinawa (in Japan) as the invariant regions. When examining the candidate calibration regions, although many areas looked white, we decided to choose these three regions based also on the following considerations: first, these three regions are located in different geographic areas around the world and have worldwide representation; second, each region has a wide spread of digital number values from very low to very high, which would improve the accuracy of the intercalibration model; third, because all are far away from the mainland and are relatively isolated, they are rarely affected by night-time light from other regions.

3.2. Intercalibration

We used the selected invariant regions as the mask, extracting the invariant area of the pending images and reference image, reading the greyscale matrices of each region, and depositing them in arrays. We then performed regression analysis of the arrays corresponding to the pending images and reference image, framed the regression model, and acquired the intercalibration models corresponding to each pending image.

A comparison of the R^2 value of the five regression models (exponential, linear, logarithmic, quadratic, and power), as shown in Figure 3, shows that the power model best fits the data series.

In this article, we use the power function to establish the regression model:

$$\mathrm{DN}_c + 1 = a \times (\mathrm{DN}_m + 1)^b, \tag{1}$$

where DN_c is the grey value after intercalibration, DN_m is the grey value before intercalibration, and a and b are model coefficients; to avoid the base number being zero, all grey values are plus one.

When employing intercalibration models that correspond to each image to correct the whole figure, the regions of value zero are excessive. Because these regions represent the

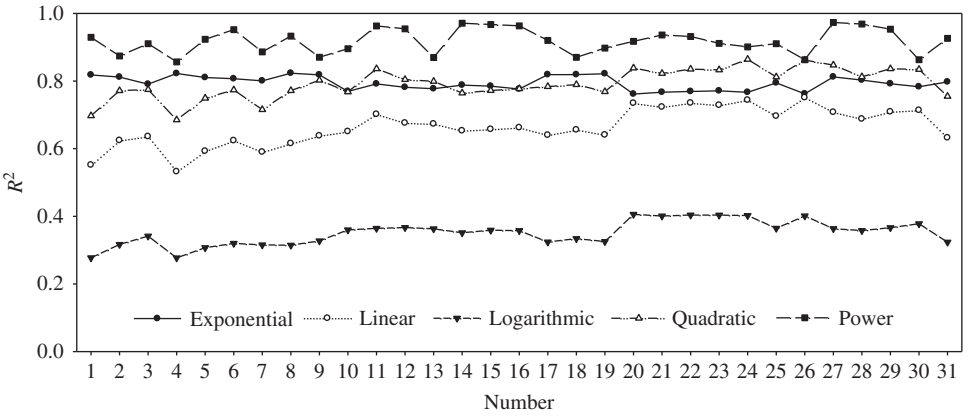

Figure 3. R^2 of the five regression models.

non-lit area, when the intercalibration model is established, they should be removed during the panorama intercalibration process.

3.3. Accuracy assessment

The most direct method of evaluation is contrasting the visual effects of images before and after intercalibration, but because it is somewhat subjective, we need a quantitative comparison. In this article, we established the evaluation index by constructing a light index (total light index, TLI), which represents the sum of the grey values in an area and can be expressed as

$$\mathrm{TLI} = \sum_i \mathrm{DN}_i \times C_i, \tag{2}$$

where DN_i is the grey value of i-level pixels and C_i is the number of i-level pixels.

Relative radiometric calibration should be able effectively reduce the differences between data in the same year from two satellites, and thereby stabilize the inter-annual variability of the same satellite. In this article, the normalized difference index (NDI) is taken as the evaluation criterion and can be expressed as follows:

$$\mathrm{NDI} = \frac{|\mathrm{TLI}_1 - \mathrm{TLI}_2|}{\mathrm{TLI}_1 + \mathrm{TLI}_2}, \tag{3}$$

where TLI_1 and TLI_2 are the total light indices of two satellite images in a certain year. The lower the NDI, the smaller the relative gap between the two images and the better the calibration result we produce.

Meanwhile, many studies on the relationship between GDP statistics and night-time light data have been conducted (Raupach, Rayner, and Paget 2010; Elvidge et al., "Relation between Satellites," 1997; Elvidge, Imhoff, et al. 2001), and their authors have reached the unanimous conclusion that there is a significant linear relationship between the two kinds of data. Therefore, we chose GDP statistics to perform linear regression with the night-time light data in this article. By comparing the fitting accuracy before and after intercalibration, we can verify the reliability of the intercalibration results.

4. Results

The calculated intercalibration model coefficients of each phase of the images are shown in Table 2.

The intercalibration results are shown in Figures 4, 5, and 6. For comparison purposes, we have also included the results from Elvidge et al.'s (2014) intercalibration, developed for stable light product. In Figure 4, the abscissa represents different years, the vertical axis represents the light index (TLI), and the curve represents the inter-annual variability of TLI value in each satellite image. Figure 5(*a*) compares the distribution of the global NDI values before and after intercalibration in the year 1994 and from 1997 to 2007. Figures 5(*b*) and (*c*) compare the intercalibration results of this article to the uncorrected results and intercalibration results of Elvidge et al. (2014), respectively. Figure 6 shows the changes in inter-annual TLI value before and after intercalibration in China, Brazil, and Egypt, and comparison with Elvidge et al.'s (2014) intercalibration results.

Figure 7 compares the linear regression results of global GDP with the TLI value in the time series from 1992 to 2010. Figure 8 shows the comparison of the R^2 value obtained from linear regression of the national GDP with the TLI value in the cross-sectional data.

Table 2. Intercalibration model coefficients of each image.

No.	Satellite	Year	*a*	*b*	R^2
1	F10	1992	0.8959	1.0310	0.9492
2	F10	1993	0.6821	1.1181	0.8731
3	F10	1994	0.9127	1.0640	0.9112
4	F12	1994	0.4225	1.3025	0.8559
5	F12	1995	0.3413	1.3604	0.9275
6	F12	1996	0.9247	1.0576	0.9541
7	F12	1997	0.3912	1.3182	0.9042
8	F12	1998	0.9734	1.0312	0.9125
9	F12	1999	1.2743	0.9539	0.8846
10	F14	1997	1.3041	0.9986	0.8945
11	F14	1998	0.9824	1.1070	0.9589
12	F14	1999	1.0347	1.0904	0.9479
13	F14	2000	0.9885	1.0702	0.9047
14	F14	2001	0.9282	1.0928	0.9706
15	F14	2002	0.9748	1.0857	0.9752
16	F14	2003	0.9144	1.1062	0.9156
17	F15	2000	0.8028	1.0855	0.9242
18	F15	2001	0.8678	1.0646	0.8700
19	F15	2002	0.7706	1.0920	0.8854
20	F15	2003	0.9852	1.1141	0.9544
21	F15	2004	0.8640	1.1671	0.9352
22	F15	2005	0.5918	1.2894	0.9322
23	F15	2006	0.9926	1.1226	0.9145
24	F15	2007	1.1823	1.0850	0.9041
25	F16	2004	0.7638	1.1507	0.9123
26	F16	2005	0.6984	1.2292	0.8620
27	F16	2006	0.9028	1.1306	0.9412
28	F16	2007	0.8864	1.1112	0.9576
29	F16	2008	0.9971	1.0977	0.9653
30	F16	2009	1.4637	0.9858	0.8735
31	F18	2010	0.8114	1.0849	0.9542

Note: All regressions are significant at the 0.01 level.

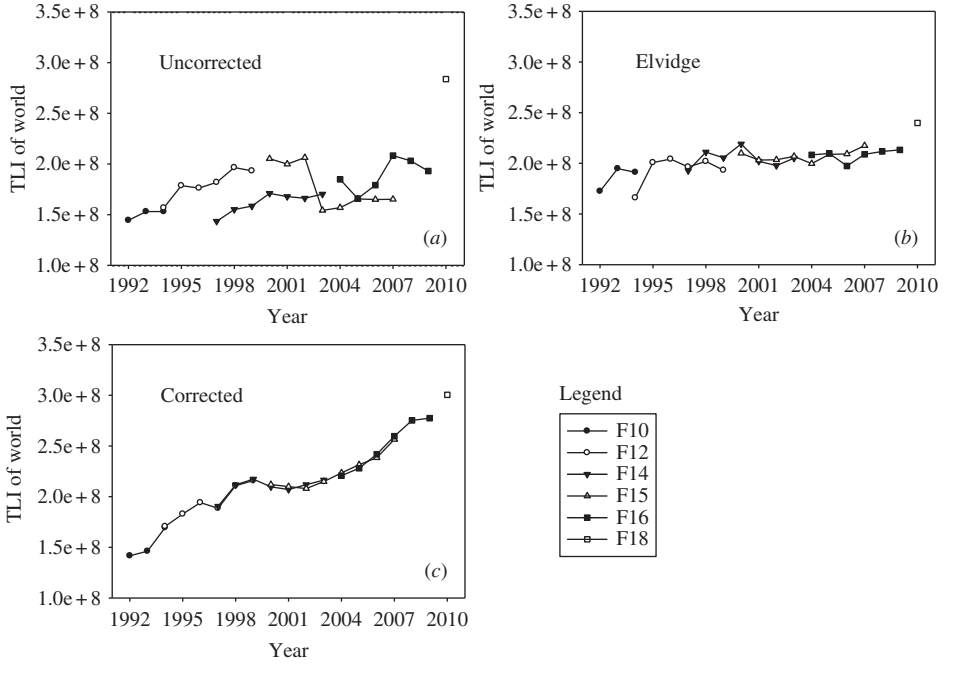

Figure 4. Contrast in global TLI after intercalibration by Elvidge et al. and the invariant region method, (*a*) uncorrected; (*b*) results from Elvidge et al.; (*c*) corrected in this article.

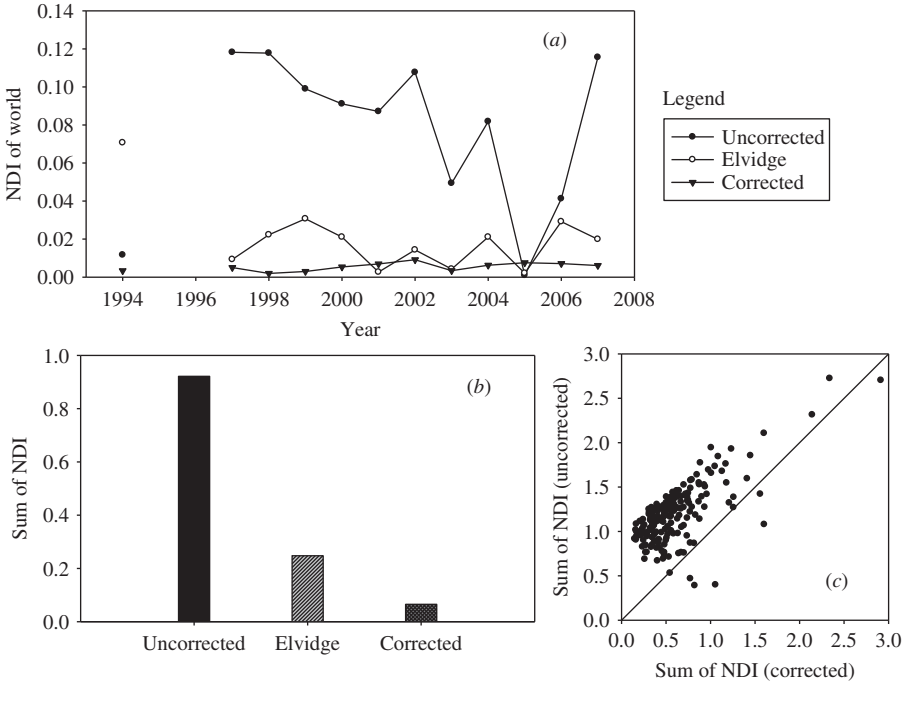

Figure 5. Contrast in global NDI after intercalibration by Elvidge et al. and the invariant region method, (*a*) contrast in time series; (*b*) contrast in sum of NDI; (*c*) scatter plot of uncorrected vs. corrected.

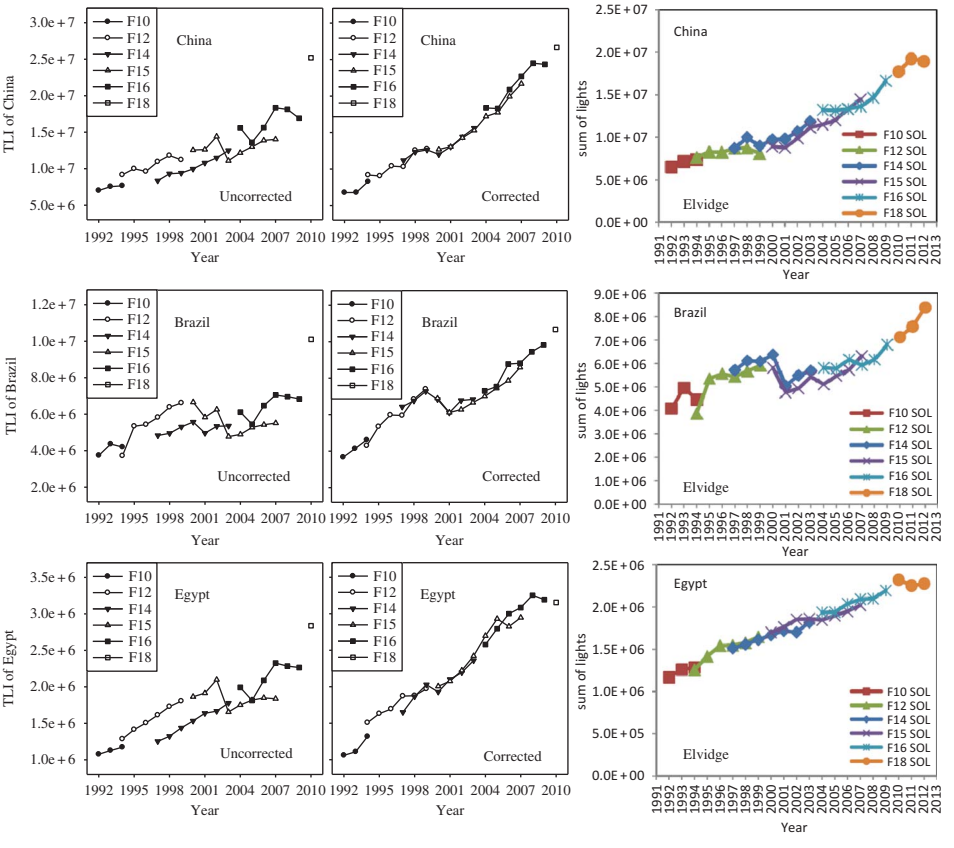

Figure 6. Contrast of several countries' TLI after intercalibration by Elvidge et al. and the invariant region method.

5. Discussion

In Figure 4(*a*), there is a large gap between data for the same year from different satellites before intercalibration, while the data from the same satellite show a strong stochastic volatility in inter-annual variability. Figure 4(*b*) shows that the intercalibration results of Elvidge et al. (2014) are most persuasive. The gap between data for the same year from different satellites has been narrowed, and there is a trend in inter-annual variability of data from the same satellite. However, the pixel saturation of the selected reference image F121999 has not been corrected, which is manifested as stability in inter-annual variability between 1992 and 2010. However, because the global economy has developed rapidly in the last 20 years, night-time light area and brightness have generally increased and such stability seems irrational. Figure 4(*c*) shows the intercalibration results of the invariant region method. Comparing these results with those of Elvidge et al. (2014), the gap between data in the same year from different satellites becomes much smaller, and the trend in inter-annual variability of the data from the same satellite becomes more obvious. In addition, since the selected reference image has no saturation, the calibrated images tend to complete the saturation correction; thus, the trend is seen to be strongly stable in the entire time series. In fact, developing a regression analysis on the basis of a non-saturated radiance-calibrated image does not change the frequency distribution of pixel values, indicating that our approach helps to reduce the impacts resulting from saturation.

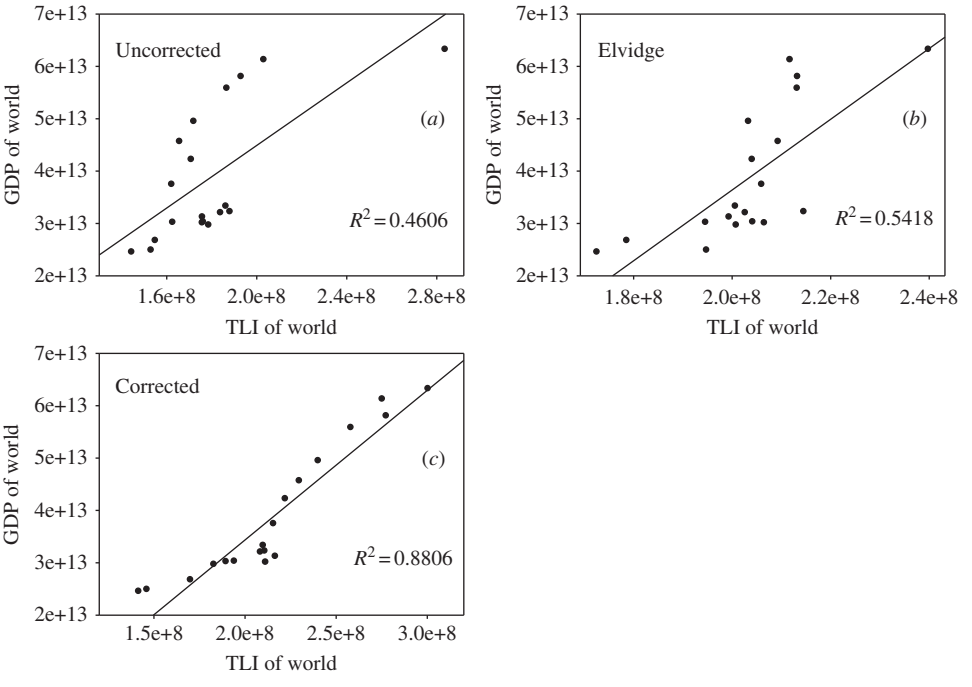

Figure 7. Comparison of the linear regression results of global GDP with TLI in the time series, (*a*) uncorrected; (*b*) results from Elvidge et al.; (*c*) corrected in this article.

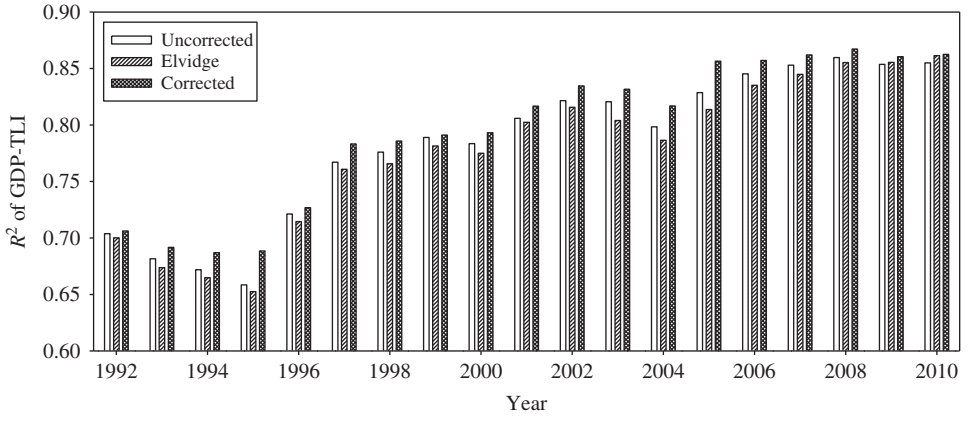

Figure 8. Comparison of the R^2 obtained from the linear regression of the national GDP with TLI in the cross-sectional data.

Over the 12 years studied (1994 and 1997–2007), this set of data was supplied by two satellites only. By contrasting the NDI of the two satellites for each year in Figure 5(*a*) and the NDI sum over the 12 years in Figure 5(*b*), we found that the results of the invariant region method turned out to be lower than the intercalibration results of Elvidge et al. (2014). In Figure 5(*c*), the horizontal axis represents each country's NDI sum after correction and the vertical axis represents the uncorrected value. Nearly 200 countries' distributions are collated in the upper part of the $y = x$ straight line; thus, we can conclude that

the intercalibration method provided in this article is effective for most countries around the world. However, the result also indicates that this intercalibration model is less applicable to a few countries and regions: small islands in the ocean, inaccessible areas, or city states, such as Antarctica, Comoros, Malta, Monaco, etc. Thus, they are temporarily not within the scope of concern in this article. Figure 6 shows the comparison of data for China, Brazil, and Egypt before and after intercalibration. It illustrates that intercalibration results at the national level are also impressive. In comparson with Elvidge et al's. (2014) calibration results, we found higher TLI values and wider ranges for the three concerned countries. We believe this is due to the fact that our reference image was a non-saturated radiance-calibrated image.

Figures 7 and 8 show the testing of intercalibration accuracy of night-time light data with GDP statistics. The test results in Figure 7 show that intercalibration significantly improved the analysis for night-time light in the time series. However, Figure 8 shows that intercalibration improved the R^2 value of the regression analysis to some extent in cross-sectional data at the national level, which indicates that the calibrated night-time light data can well characterize GDP or other applications. In addition, from Figure 8, we also see that the most recent data have higher precision, which may be related to the development of satellites and sensors.

Since many studies on the relationship between night-time light data and GDP have been carried out, and all have reached the same conclusion that the two have a significant linear relationship, the method of testing data accuracy with GDP is reliable in this article.

In this method, selecting the invariant regions is vulnerable to the subjective cognition: that is, different selections produce different results. In addition, intercalibration models may also have other options. Therefore, the question of whether the power function model based on regression analysis fitting is optimal requires further study. Moreover, since the method is based on statistical theory, the results are more reliable and accurate in large-scale regional studies if we employ the above-mentioned TLI as the evaluation criterion. However, there may be large errors if the study area is small and only a small number of pixels are involved. To avoid such errors, we need to use more parameters (e.g. surface reflectance when the satellite transits, atmospheric visibility, solar zenith angle, and satellite sensor calibration parameters) for absolute radiometric calibration. Nevertheless, absolute radiometric calibration is very difficult, as its required parameters are not easy to obtain, and the cost of the work is considerably high.

To reduce errors caused by data saturation, some scholars (Sutton 2003; Cheng 2008), who held that a logarithm could flatten the variation in data series so that it can reduce the errors caused by data saturation, processed logarithmic transformation on the data. However, in this article, it is considered both inappropriate and inaccurate because log processing will change the linear relationship between light data and socio-economic data.

6. Conclusions

In this article, we present an alternative strategy to apply the invariant region method for improving the intercalibration model of DMSP-OLS night-time light data. Compared with the intercalibration method supplied by Elvidge et al. (2014), the invariant region method can carry out both relative radiometric calibration and saturation correction and can reduce the errors caused by inter-annual variation and pixel saturation. The intercalibration accuracy of this method turned out to be very good on global, national, and regional scales.

Using the corrected data to estimate the socio-economic data of countries and regions lacking statistical information is a new method. Compared with anthropogenic statistics, night-time light data is more objective, rapid, and less expensive; it can provide governments with rapid insight into the real global distribution of socio-economic status, so that they can formulate or adjust their political and economic strategies. Additionally, night-time light data are a reflection of the natural distribution of night light on the ground, but the statistics are based on the administrative region unit and thus cannot be implemented within a natural area. Therefore, we can employ the grey value of night light as a measure to spatialize socio-economic factors, so that the socio-economic data can be implemented into a natural block, allowing for more sophisticated and accurate research.

Therefore, we believe that calibrated data processed by the invariant region method can greatly enhance the accuracy of future research work, such as carbon emissions calculation, GDP statistics verification, spatial population, resources and environment management, etc.

Acknowledgements

This work was supported by the National Natural Science Foundation of China (No. 41271101 and No. 41130534).

References

Amaral, S., A. Monteiro, G. Camara, and J. A. Quintanilha. 2006. "DMSP/OLS Night-Time Light Imagery for Urban Population Estimates in the Brazilian Amazon." *International Journal of Remote Sensing* 27: 855–870.

Chand, T., K. Badarinath, C. D. Elvidge, and B. T. Tuttle. 2009. "Spatial Characterization of Electrical Power Consumption Patterns over India Using Temporal DMSP-OLS Night-Time Satellite Data." *International Journal of Remote Sensing* 30: 647–661.

Chaturvedi, M., T. Ghosh, and L. Bhandari. 2011. "Assessing Income Distribution at the District Level for India Using Nighttime Satellite Imagery." In *Proceedings of the 32nd Asia-Pacific Advanced Network Meeting*, 192–217. New Delhi, August 22–26.

Cheng, L. Y. 2008. "Spatial and Temporal Analysis of Population Distribution in China Using DMSP/OLS Nightlight Emissions Data." Master thesis, Institute of Remote Sensing Applications, Chinese Academy of Sciences, Beijing (in Chinese).

Coppin, P. R., and M. E. Bauer. 1994. "Processing of Multitemporal Landsat TM Imagery to Optimize Extraction of Forest Cover Change Features." *IEEE Transactions on Geoscience and Remote Sensing* 32: 918–927.

Doll, C., J. P. Muller, and J. G. Morley. 2006. "Mapping Regional Economic Activity from Night-Time Light Satellite Imagery." *Ecological Economics* 57: 75–92.

Elvidge, C. D., K. E. Baugh, E. A. Kihn, H. W. Kroehl, and E. R. Davis. 1997. "Mapping City Lights with Nighttime Data From the DMSP Operational Linescan System." *Photogrammetric Engineering and Remote Sensing* 63: 727–734.

Elvidge, C. D., K. E. Baugh, E. A. Kihn, H. W. Kroehl, E. R. Davis, and C. W. Davis. 1997. "Relation between Satellites Observed Visible-Near Infrared Emissions, Population, Economic Activity and Electric Power Consumption." *International Journal of Remote Sensing* 18: 1373–1379.

Elvidge, C. D., K. E. Baugh, P. C. Sutton, B. Bhaduri, B. T. Tuttle, T. Ghosh, D. Ziskin, and E. H. Erwin. 2011. "Who's in the Dark: Satellite Based Estimates of Electrification Rates." In *Urban Remote Sensing: Monitoring, Synthesis and Modeling in the Urban Environment*, edited by X. Yang, 211–224. Chichester: John Wiley & Sons.

Elvidge, C. D., V. R. Hobson, K. E. Baugh, J. B. Dietz, Y. E. Shimabukuro, T. Krug, E. Novo, and F. R. Echavarria. 2001. "DMSP-OLS Estimation of Tropical Forest Area Impacted by Surface Fires in Roraima, Brazil: 1995 versus 1998." *International Journal of Remote Sensing* 22: 2661–2673.

Elvidge, C. D., F. C. Hsu, K. E. Baugh, and T. Ghosh. 2014. "National Trends in Satellite Observed Lighting: 1992–2012." In *Global Urban Monitoring and Assessment Through Earth Observation*, edited by Q. Weng. Boca Raton, FL: CRC Press.

Elvidge, C. D., M. L. Imhoff, K. E. Baugh, V. R. Hobson, I. Nelson, J. Safran, J. B. Dietz, and B. T. Tuttle. 2001. "Night-Time Lights of the World: 1994–1995." *ISPRS Journal of Photogrammetry and Remote Sensing* 56: 81–99.

Elvidge, C. D., J. Safran, B. Tuttle, P. Sutton, P. Cinzano, D. Pettit, J. Arvesen, and C. Small. 2007. "Potential for Global Mapping of Development via a Nightsat Mission." *GeoJournal* 69: 45–53.

Elvidge, C. D., P. C. Sutton, T. Ghosh, B. T. Tuttle, K. E. Baugh, B. Bhaduri, and E. Bright. 2009. "A Global Poverty Map Derived From Satellite Data." *Computers & Geosciences* 35: 1652–1660.

Elvidge, C. D., D. Ziskin, K. E. Baugh, B. T. Tuttle, T. Ghosh, D. W. Pack, E. H. Erwin, and M. Zhizhin. 2009. "A Fifteen Year Record of Global Natural Gas Flaring Derived from Satellite Data." *Energies* 2: 595–622.

Gallo, K. P., J. D. Tarpley, A. L. Mcnab, and T. R. Karl. 1995. "Assessment of Urban Heat Islands: A Satellite Perspective." *Atmospheric Research* 37: 37–43.

Ghosh, T., R. Powell, C. D. Elvidge, K. E. Baugh, P. C. Sutton, and S. Anderson. 2010. "Shedding Light on the Global Distribution of Economic Activity." *The Open Geography Journal* 3: 147–160.

Hall, F. G., D. E. Strebel, J. E. Nickeson, and S. J. Goetz. 1991. "Radiometric Rectification: Toward a Common Radiometric Response Among Multidate, Multisensor Images." *Remote Sensing of Environment* 35: 11–27.

Lenney, M. P., C. E. Woodcock, J. B. Collins, and H. Hamdi. 1996. "The Status of Agricultural Lands in Egypt: The Use of Multitemporal NDVI Features Derived from Landsat TM." *Remote Sensing of Environment* 56: 8–20.

Liu, Z. F., C. Y. He, and Y. Yang. 2011. "Mapping Urban Areas by Performing Systematic Correction for DMSP/OLS Nighttime Lights Time Series in China from 1992 to 2008." In *Geoscience and Remote Sensing Symposium (IGARSS), 2011 IEEE International*, 1858–1861, Vancouver, July 24–29.

Lo, C. P. 2001. "Modeling the Population of China Using DMSP Operational Linescan System Nighttime Data." *Photogrammetric Engineering and Remote Sensing* 67: 1037–1047.

Lo, C. P. 2002. "Urban Indicators of China from Radiance-Calibrated Digital DMSP-OLS Nighttime Images." *Annals of the Association of American Geographers* 92: 225–240.

McDonald, R. I., P. Kareiva, and R. T. T. Formana. 2008. "The Implications of Current and Future Urbanization for Global Protected Areas and Biodiversity Conservation." *Biological Conservation* 141: 1695–1703.

Raupach, M. R., P. J. Rayner, and M. Paget. 2010. "Regional Variations in Spatial Structure of Nightlights, Population Density and Fossil-Fuel CO_2 Emissions." *Energy Policy* 38: 4756–4764.

Sutton, P. C. 2003. "A Scale-Adjusted Measure of 'Urban Sprawl' Using Nighttime Satellite Imagery." *Remote Sensing of Environment* 86: 353–369.

Sutton, P. C., C. D. Elvidge, and T. Ghosh. 2007. "Estimation of Gross Domestic Product at Sub-National Scales Using Nighttime Satellite Imagery." *International Journal of Ecological Economics and Statistics* 8: 5–21.

Zhang, P. Q., X. C. Yu, Z. Liu, J. S. Li, and G. Wan. 2006. "A Study on Relative Radiometric Correction of Multitemporal Remote Sensing Images." *Journal of Remote Sensing* 10: 339–344 (in Chinese).

Zhao, N. Z., T. Ghosh, and E. L. Samson. 2012. "Mapping Spatio-Temporal Changes of Chinese Electric Power Consumption Using Night-Time Imagery." *International Journal of Remote Sensing* 20: 6304–6320.